PREDICTION OF FLOW FIELD IN A 180 DEG CHANNEL

Yuu Itai, yuuitai@ufpa.br
EBMA, Departamento de Engenharia Mecânica – Universidade Federal do Pará, Belém – Pará, CEP 66075-110.

Danielle R. S. Guerra, daguerra@ufpa.br
EBMA, Departamento de Engenharia Mecânica – Universidade Federal do Pará, Belém – Pará, CEP 66075-110.

Daniel O. A. Cruz, doac@ufpa.br
Departamento de Engenharia Mecânica – Universidade Federal do Pará, Belém – Pará, CEP 66075-110.

Abstract: *Flows with three-dimensional effects are found in turbo machines and around complex bodies. These effects can be produced by a channel with curved walls that provides curvature or changes on the direction of the streamlines. The experimental study of the three-dimensionality and the structure of the turbulent flows, usually requires optical techniques like the laser-Doppler anemometry or particle image velocimetry systems, PIV. However, high costs of the experimental apparatus associated with these methods make these techniques inaccessible to many laboratories. Turbulent flows with streamline curvature are on considerable engineering interest. The aim of this work is describing the behavior of the turbulent air flow in a curved channel through the analysis of the three dimensional effects using the commercial code FLUENT 6.0. The objective is providing a preliminary study for a future investigation in flow around blades. Three turbulence models were applied to obtain the mean velocity field, vorticity and pressure gradients. In this study the grid of the geometry was developed from dimensions of the wind tunnel located at the Fluid Mechanics Laboratory – DEM/UFPA. The wind tunnel has a curved rectangular test section of 150x300mm, with a fully developed channel flow.*

Keywords: *curved channel, streamline, vorticity, velocity*.

1. INTRODUCTION

Computational fluids dynamics codes used to simulate cases have had an important place among the methods analysis and structures construction. Although it is necessary the knowledge of what appropriate model had been used in our case. Is completely necessary the using of commercial codes because the expensive costs of optical equipment adopted to measure the three-dimensional effects and draining structure turbulence. These variables usually require the using of optic techniques as anemometry for Laser-Doppler or attainment systems of the field of speed for particle image, PIV, and it represents a problem when doesn't have a lot of investments becoming practically inaccessible to some laboratories.

Shao et al. (2002) developed a simulation model which uses Reynolds averages, 3D Navier Stokes equations based on a boundary-fitted orthogonal curvilinear coordinate system. Two approaches for equation system closure are used, i.e, algebric stress models and nonlinear k - ε model for eddy viscosity. The different closure approaches have been discussed and the model was validated using measurements in curved rectangular channels. Predicted turbulence and secondary flow patterns in curved compound channel were compared with straight channels measurements.

Kim et al. (1994) investigated the developing turbulent flow in a 90 deg curved duct of rectangular cross section, and an aspect radio of 6 was also investigated. The mean-velocity was measured with a five-hole pressure probe and Reynolds-stress components was measured with two sensors hot-wire probes, in the boundary layers on the duct walls to document the pressure driven secondary motion and the formation of a longitudinal vortex near the corner in the convex wall.

Shima et al. (2000), tested a low-Reynolds-number second-moment closure without wall-reflection redistribution terms in wall-bounded turbulent flows with streamline curvature. The turbulence model was previously shown to give good predictions for a fully developed channel flow, adverse and favorable pressure gradients, plane and round jets, and flows with wall blowing and suction and other good predictions. The model is used to calculate two fully developed curved channel flows and four boundary layers on curved walls. The turbulence model captures main features of the stabilizing and destabilizing effects of streamline curvature, though some notable discrepancies between the predictions and measurements are present in boundary layers on convex walls.

Silva et al. (1998) has an objective and good explanation to turbulence phenomenon and their variants.

Treaster et al. (1979) has developed programs to calibrate and employ five-hole probes of both angle tube and prismatic geometries and discuss about the applications.

Iacovides et al. (1990) has reported a computational and experimental study of turbulent flow around a square-sectioned U-bend. All velocities measurements were obtained with DISA and TSI constant-temperature, hot-wire anemometers using standard DANTEC single and cross-wire probes. The flow prediction was studied using a software including the turbulence model.

Humphrey et al (1981) investigated steady, incompressible, isothermal developing flow in a square-section curved (comprises a 90° perpex bend) duct with smooth walls. The measurements (the longitudinal and radial components of

mean velocity and corresponding components of the Reynolds stress tensor) were obtained with a Laser Doppler anemometer. Calculated mean velocity results obtained from solution of elliptic differential equations in finite difference form and incorporating a two-equation turbulence model are not strongly dependent on the model.

Schlichting (1968) presents the explanation of sprouting, development and separation of boundary layer. With a different way these studies insert values to this work.

The documentation of commercial code FLUENT 6.0 (2005) explains very well the equations of transport and turbulent models. What the appropriated cases to apply the turbulence model and the restrictions and vantages of all the models.

The present paper compare three turbulence models inserted on the commercial code FLUENT 6.0 analyzing their performance during the air draining in a wind tunnel, located at the Fluid Mechanics Laboratory – DEM/UFPA. The wind tunnel has a curved rectangular test section of 150x300mm, with a fully developed channel flow.

2. CASE FORMAT

The mesh was created in the commercial code GAMBIT 2.0, that was developed to create geometry and meshes, where a boundary layer was developed to facilitate the calculations refining the places close to the wall. The mesh was constructed with a growth factor of 0.005 and B/A tax of 1.055 to the part that contain the curvature and the rectangular part. The structure has been shared in three parts becoming easier to create the boundary layer and the mesh. Two rectangular parts were meshed with 0.025 of size on the HEX MAP mode and the curvature with 0.008 on the same mode of the rectangular parts.

Two zones have been defined, the entrance with velocity inlet and the exit with pressure outlet. We have to point out the way that the structure will be meshed. It is highly important when the calculation runs to converge. The order of mesh command to elements also has been discussed since then each structure has a different way to apply and create the perfect mesh. The first volume presents 15400 elements and 17388 nodes, the second part, that represents the curve, had 179200 elements and 194292 nodes and the third part contains 18200 elements and 20412 nodes, totalizing 212800 elements and 230580 nodes. Figure 1 shows the structure of curvature presents at the wind tunnel located at the Fluid Mechanics Laboratory – DEM/ UFPA.

(a)   (b)
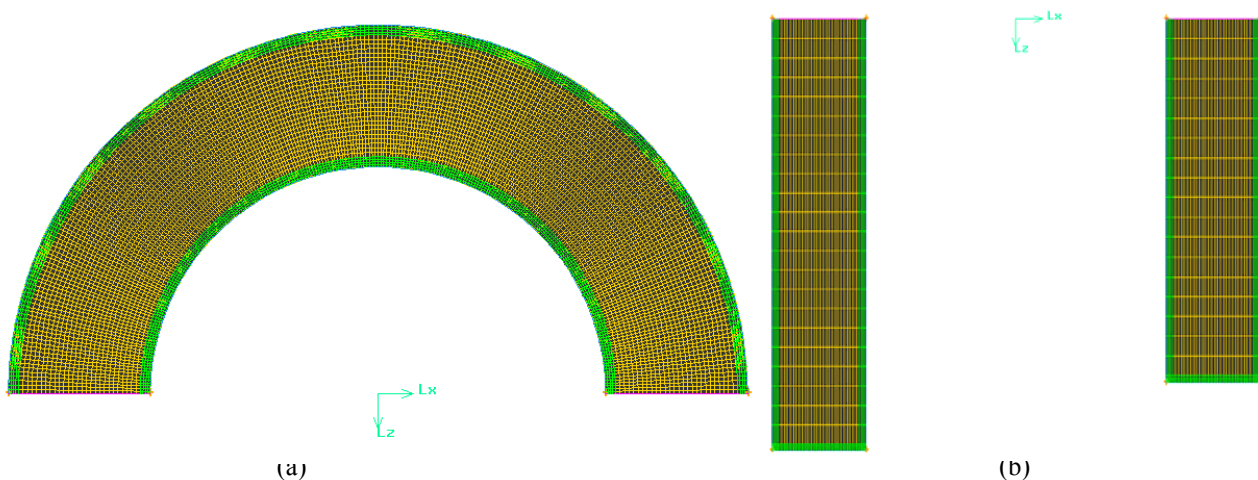
Figure 1 – (a) The grid mesh of curvature and (b) the rectangular structures presents at the wind tunnel.

Figure 2 – The wind tunnel.

On Figure 1 (b) it's shown the two rectangular structures that united at the curvature shown on Figure 1 (a) form the complete structure of wind tunnel. And on Figure 2 it's shown the real structure located at the Fluid Mechanics Laboratory – DEM/UFPA.

3. TURBULENCE MODELS

Three turbulence models have been chosen for the accomplishment of this work. The Standard $k - \varepsilon$, the RNG k - ε and the Reynolds Stress Model (RSM). This explanation is based on FLUENT 6.0 Documentation (2005). The details of turbulence models applied to predict this case are better explained in a separate paper. Only aspects that have particular relevance to the present analysis are going to be repeated here.

4. RESULTS

The simulation was conducted considering the initial velocity was 10 m/s and the outlet pressure was 101325 Pa. Using the turbulence models we compared results of velocity and pressure gradients. All models have a good convergence. Although some models results are greater than others and lately we discuss the results. We have to create six planes to show better the velocity behavior along the wind tunnel. The Fig. 3 shows where the planes are located.
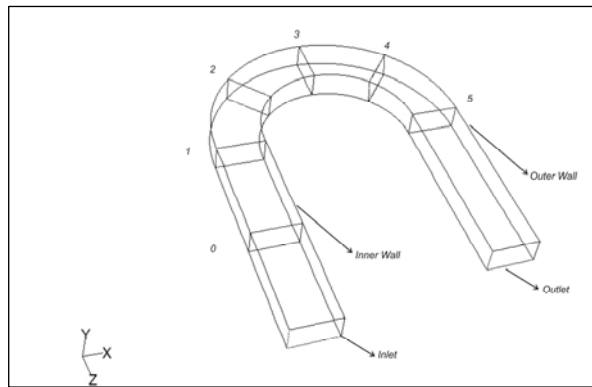
Figure 3 – The six planes created in wind tunnel with a strong curvature.

Figure 4 shows the profiles of the longitudinal velocity component, U, across de duct, from the outer to the inner wall on the six planes. The corresponding distributions of the V and W components are not shown. On plane 0, the velocity profile shows a flat plate type boundary layer. Plane 1 is the position where the curved section begins, on this plane the longitudinal velocity increase near the inner wall.

On plane 2 the longitudinal velocity increases closer to the inner wall and decreases until the outer wall. These effects are repeated in the middle of the curvature on plane 3. However, on plane 3 the longitudinal velocity near the inner wall begins to decrease.
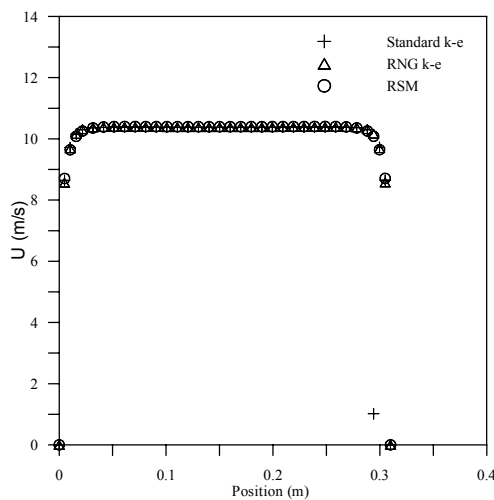
(a) Plane 0, on the middle of the first straight section.
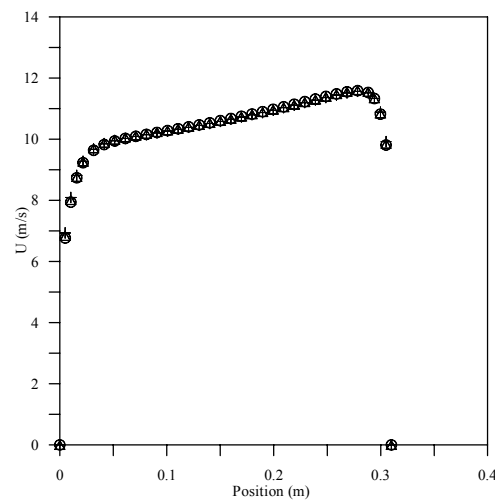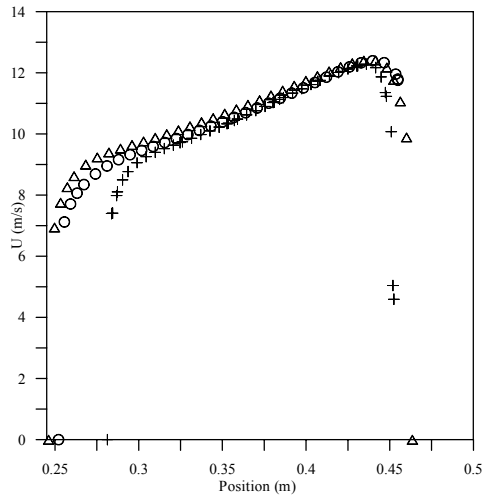
(b) Plane 1, upstream of the bend.

(c) Plane 2, on the first curvature.
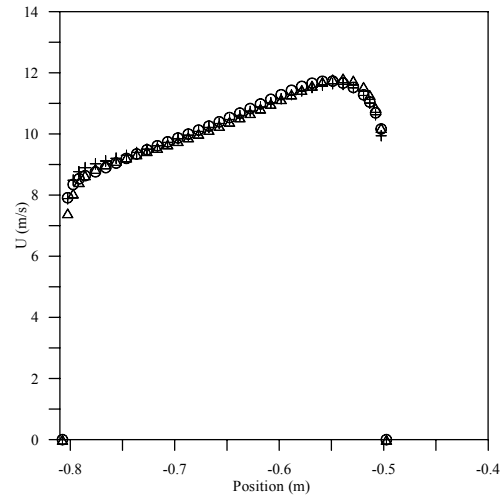
(d) Plane 3, on the middle of the curvature.
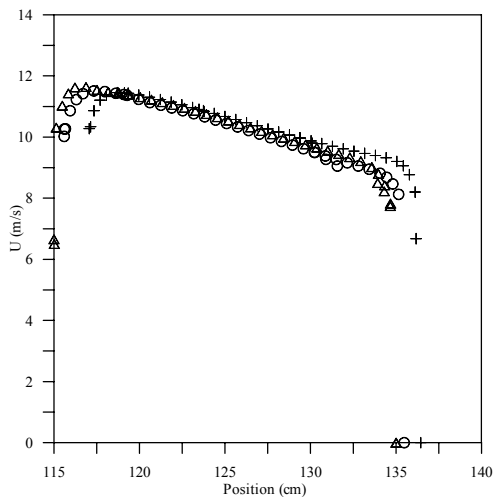
(e) Plane 4, on the second curvature.
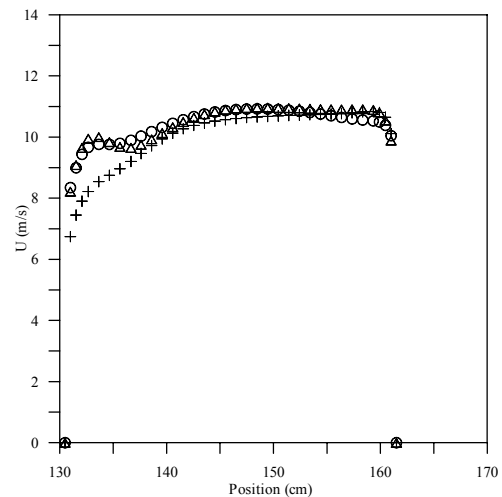
(f) Plane 5, on the exit of bend.

Figure 4 – Longitudinal velocity predicted by the three turbulent models, from outer to inner wall: (a) on plane 0, (b) on plane 1, (c) on plane 2, (d) on plane 3, (e) on plane 4 and (f) on plane 5.

On plane 4, the effect is changed, the longitudinal velocity is increased near the outer wall and presents diminish close to the inner wall. Finally, on plane 5 we can notice the presence of a longitudinal vortex through the profiles of U, which depict the two peaks commonly observed in flows with vortex. These observations are consistent with the effect of concave curvature which acts to increase turbulent mixing and leads to increase velocity close to the wall.

It was observed that the pressure distribution along the channel walls is strongly determined by the curvature. The pressure gradients induced by the curvature are clearly seen. The results of simulation indicated that on the inner wall, the boundary layer is subjected to a favorable pressure gradient starting upstream of the bend, close to the plane 1, where highest velocities are found.

According to Kim et al (1994) the flow transition of the curve for the straight line causes a reduction of the pressure in the concave wall and increase in the convex wall, generating in this last adverse gradient of pressure, propitious condition to the separation of the boundary layer.

The results for longitudinal velocity profiles predicted by the three turbulent models have shown the same behavior for all planes. On the inlet, plane 0, and upstream the bend, plane 1, all three turbulence models predicted very well the longitudinal velocity. The Standard k - ε model provided poor results for the velocity near the wall when the flow presents a strong curvature, it can be observed in the Figures 4(c) and 4(e), planes 2 and 4. On the exit of the bend, this turbulence model was not able to predict the effect of the longitudinal vortex as shown in the Figure 4 (f).

The other two turbulence models, RNG $k – \varepsilon$ and Reynolds stress model, have predicted longitudinal velocity data closer to the wall than the Standard k - ε model. These two models were able to capture the presence effect of a longitudinal vortex. This effect can be seen by the peak on the longitudinal profile in Figure 4(f).

The results below are the bidimensional planes, (x, y), on the planes 0, 1, 2, 3, 4 and 5.

In a curved duct of rectangular section it was noticed the secondary flows of first and second type, determined respectively for the bending and the section's rectangular form.

The results in Figure 5(a) and (b) have shown that in the straight section there was not secondary flow. The same behavior was seen in the vectors provided by the simulation using the RNG $k - \varepsilon$ and the RSM models, on planes 0, 1 and 3.

On plane 2 in the first curvature, the Standard $k - \varepsilon$ indicated strong inclined currents; this region presents two vortexes, one on the right side close to the inner wall, one on the top of the outer wall. On this plane is clearly seen the region of higher velocities. Again, on plane 4, in the second curvature, it can be seen inclined secondary currents; no vortex was predicted by the Standard $k - \varepsilon$ in this region.

Humphrey et al. (1981) considered that the secondary flows of first type are created from the misbalancing between the centrifugal force and the gradient of radial pressure acting on the fluid of the boundary layer of the curve's sidewalls, changing it, throughout these walls, for the internal region of the curve. The continuity demands a corresponding movement dislocating fluid, throughout the plan of symmetry, from the convex wall (internal region) to concave walls (external) of the curve, generating itself thus the two great vortices in against rotation characteristic of the draining in curved duct. And this type of secondary flow can be seen in Plane 2 and 4.

On plane 5, the model predicted an asymmetric secondary flow. In this region the higher velocities are concentrated close to the outer wall. Schlichting (1968) has explained that the secondary flows of second type occur throughout the bisector in direction to the corner, where it bifurcates and returns in opposing directions. This second type of secondary flows is weaker than the first type and it's seemed for the elongation of isolines of velocity in direction to the corner. And this type can be seen on Planes 3 and 5.

Iacovides et al (1990) has explained the secondary motion in modifying the streamwise flow. This flow is deflected down the inside wall toward the duct mid-plane and a return flow occurs from the inside to the outside over the core region of the duct.

This is the classical single-cell vortex flow that pertains at the 45-degree station. By 90 deg, the readjustments to the streamwise velocity field lead, through its coupling with the pressure fields, to the eye of the secondary vortex being pushed from far to the inside to the bend. This is what causes the development of "mushroom-shaped" velocity contours near the inner wall as the return fluid is deflected away from the center plane; indeed, it is displacement of low-momentum fluid near the center plane that is directly responsible for the "troughs". And it can be seen on the Fig. 4 (f), 5 (f), 6 (c) and 7(c).
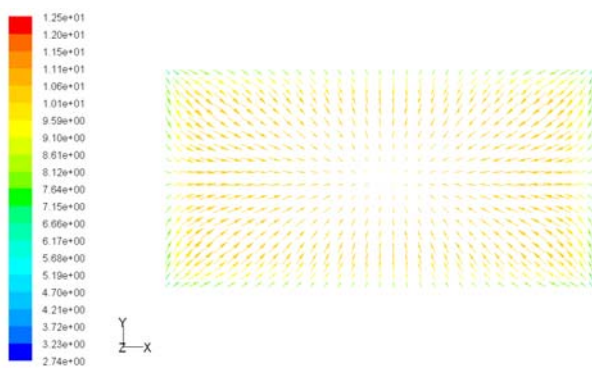
(a) Plane 0, on the middle of the first straight section.
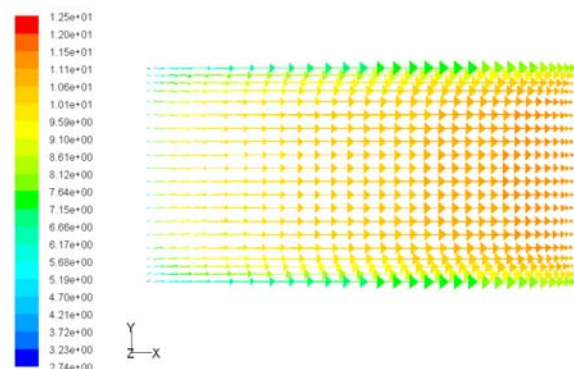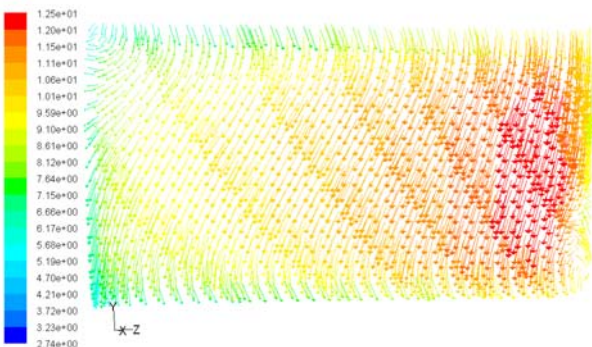
(b) Plane 1, upstream of the bend.

(c) Plane 2, on the first curvature.
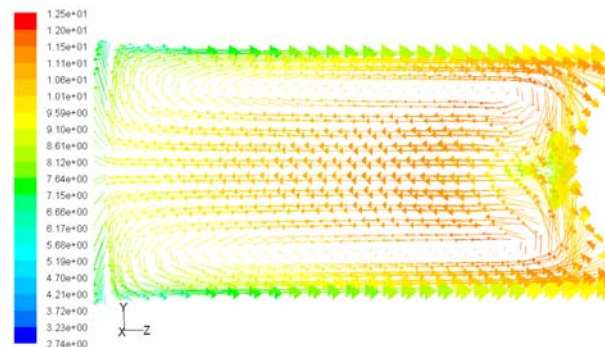
(d) Plane 3, on the middle of the curvature.
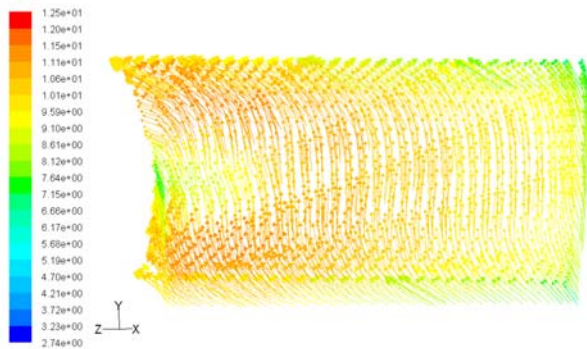
(e) Plane 4, on the second curvature.
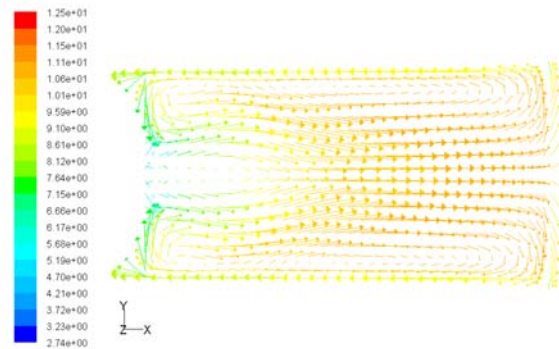
(f) Plane 5, on the exit of bend.

Figure 5 – Prediction by the Standard k - ε model on planes: (a) 0, (b) 1, (c) 2, (d) 3, (e) 4 and (f)5.
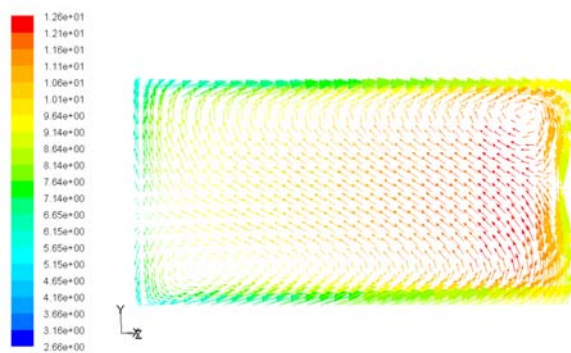
(a) Plane 2, on the first curvature.
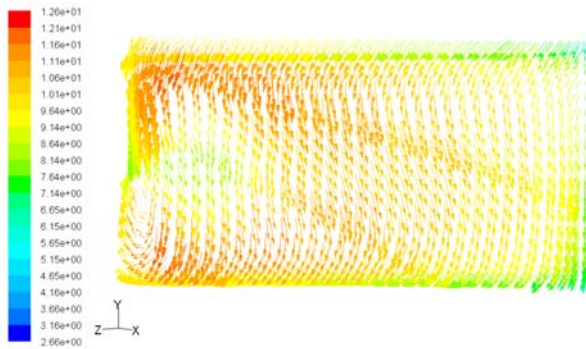
(b) Plane 4, on the second curvature.
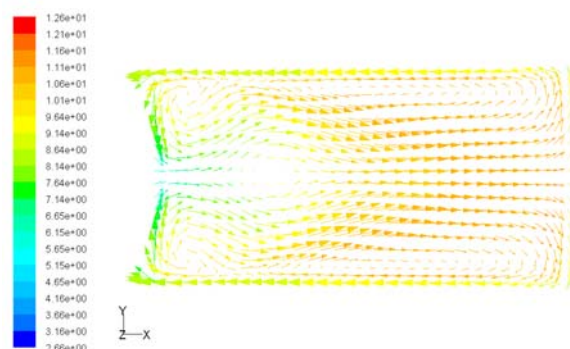
(c) Plane 5, on the exit of bend.

Figure 6 – Secondary flow predicted by the RNG $k – \varepsilon$ model on planes: (a) 2, (b) 4 and (c) 5.

Figure 6 shows the results provided by the RNG $k – \varepsilon$. These predictions were different from the predictions provided by the Standard $k – \varepsilon$. Plane 2 presents strong inclined secondary currents that forms two vortex at the opposite position of that predicted by the Standard $k – \varepsilon$.

On Plane 4 a vortex appears close to the outer wall. The same behavior predicted by the Standard $k – \varepsilon$ for the plane 5 could be seen again. However, the RNG $k – \varepsilon$ could capture the strong curvature of the streamlines and predicted the growth of two vortex close to the inner wall.

Results of the RSM are shown in Figure 7. It can be seen a similar behavior to that founded by the other turbulence models. However, there was not an agreement on the prediction of the vortex that appears on plane 2. This model could not be able to predict a vortex near the outer wall at plane 4 as seen by the results of RNG $k – \varepsilon$.
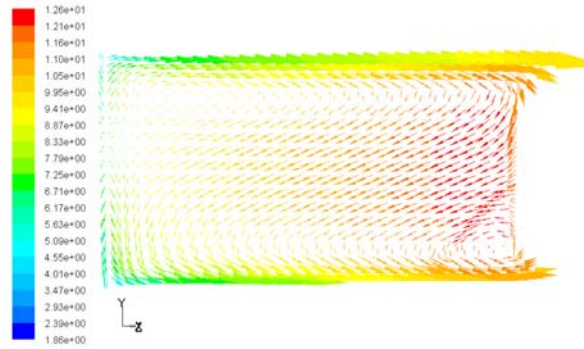
(a)   Plane 2, on the first curvature.
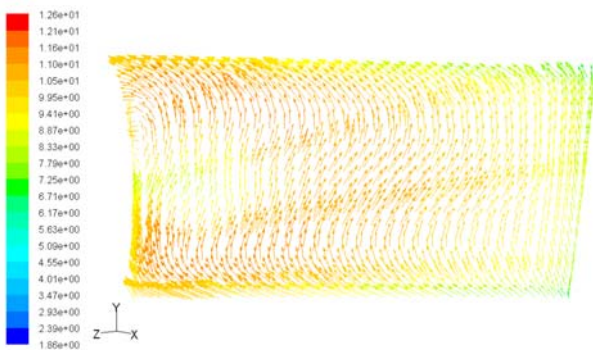
(b) Plane 4, on the second curvature.
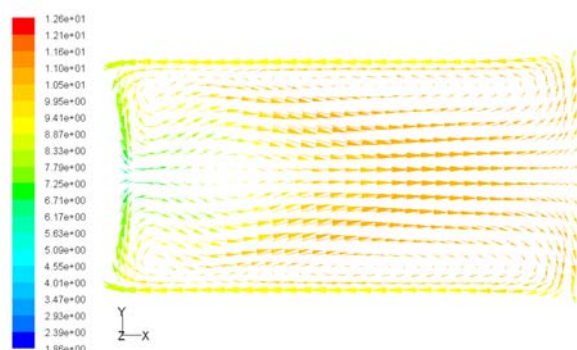
(c) Plane 5, on the exit of bend.

Figure 7 – Secondary flow predicted by the RSM: (a) on plane 2, (b) on plane 4, (c) on plane 5.
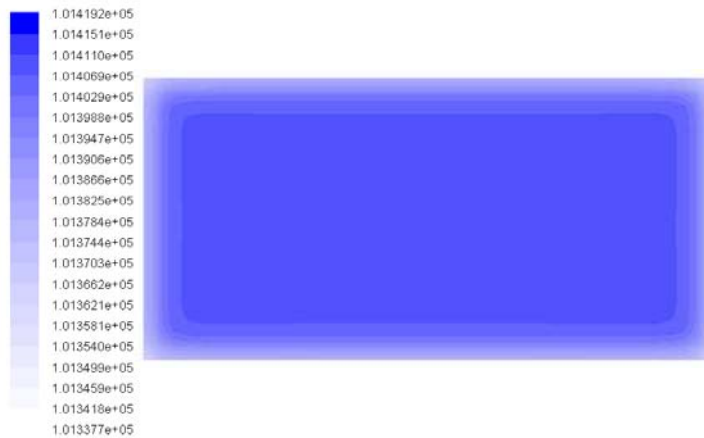
(a) Plane 0, on the middle of the first straight section.
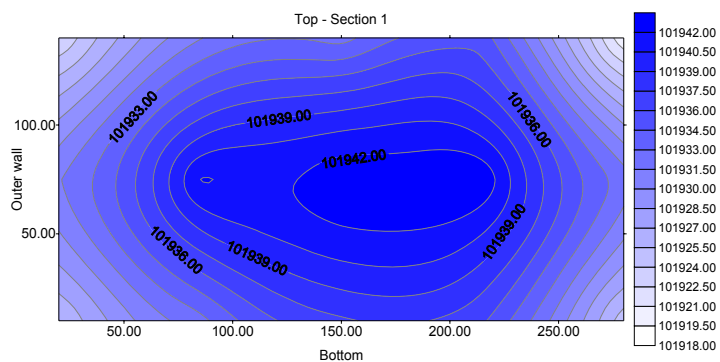
(b)
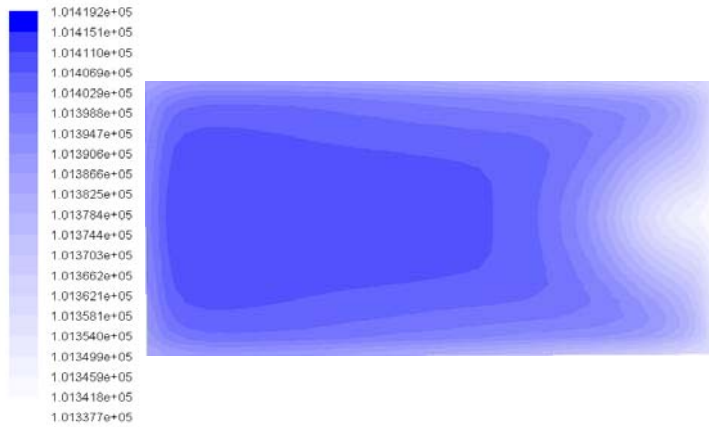
(a) Plane 3, on the middle of the curvature

(b)

(a)　　　Plane 4, on the second curvature.　　　(b)

(b)

(a) Plane 5, on the exit of bend
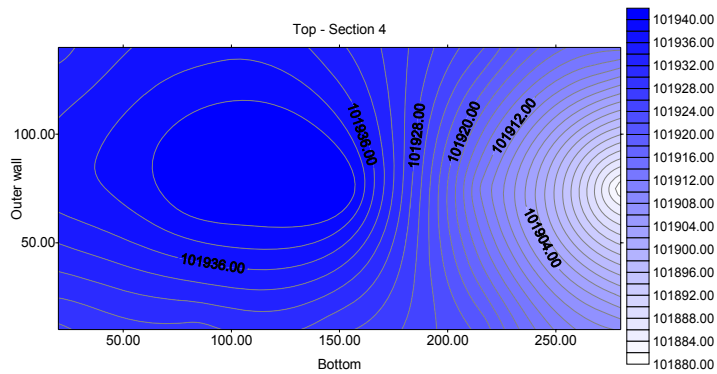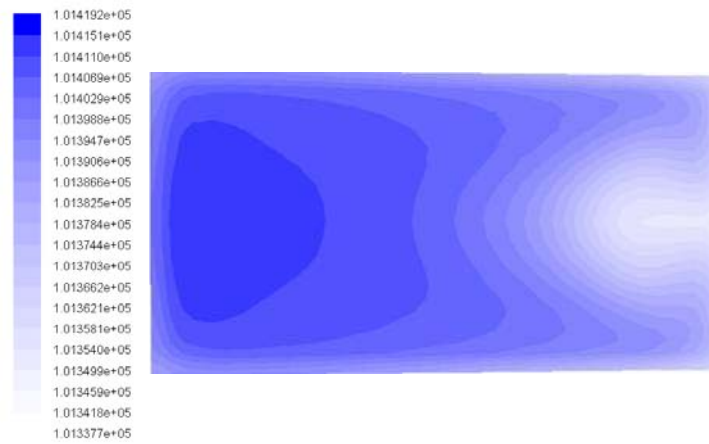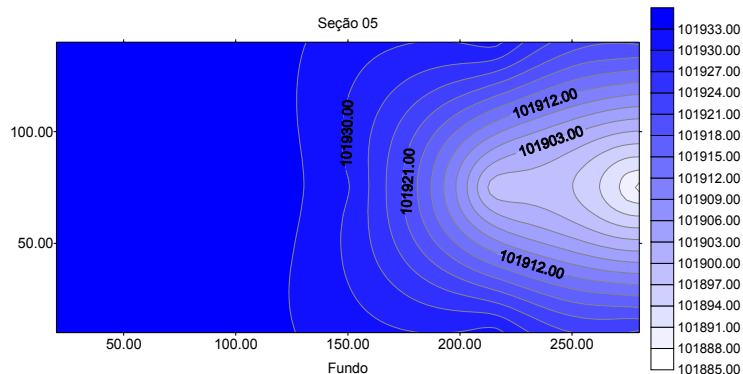
(b)
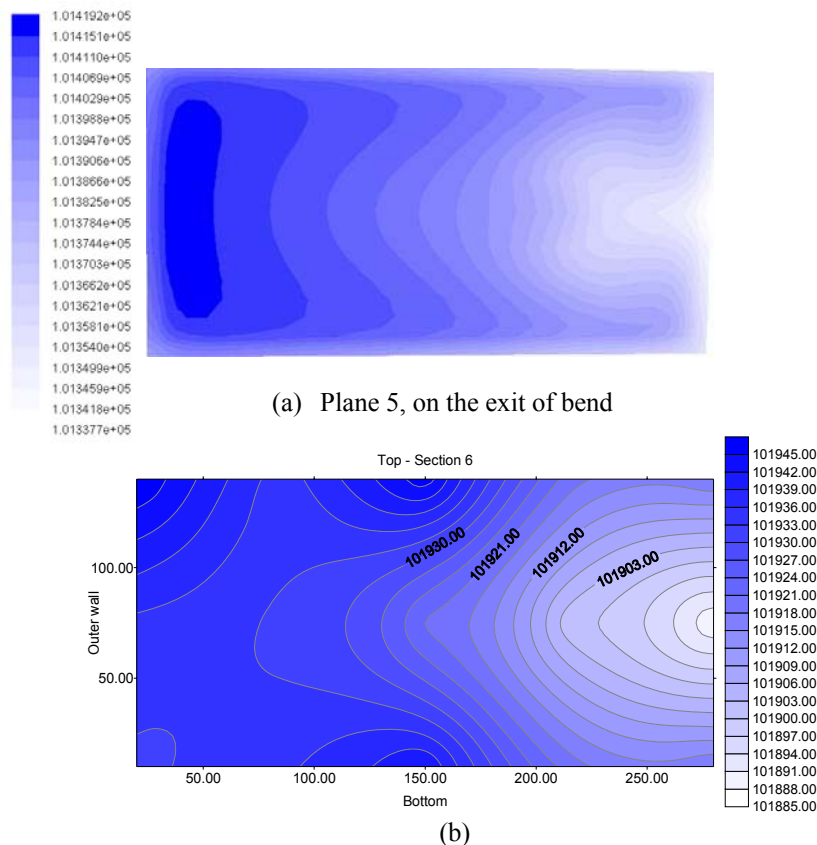
Figure 8 – The comparison between the results obtained in the numerical prediction (a) and the experimental (b).

5. CONCLUSION

Three turbulence models were tested successfully on the prediction of the longitudinal velocity and secondary flow in a curved test section of a wind tunnel. The RNG $k - \varepsilon$ model has provided better results. This model has indicated the best profile of velocity magnitude on the exit of the wind tunnel and has shown the best contour of velocity magnitude. But the profiles of the Standard $k - \varepsilon$ and the RSM model were not bad. The RNG $k - \varepsilon$ model improves the accuracy for rapidly strained and swirling flows. This characteristic of the model appears on the results of the prediction of the secondary flow. The good results provided by the RSM model are due to it is more complete than the other two models because it has more equations and has a greater potential to give accurate predictions for complex flows.

The wind tunnel flow is a little complex because of the constant values of velocity develop a profile that changes a lot during the simulation. At first is constant, in a second time is concentrated on the internal part of curvature and finally changes to opposite side and finishes with developed flow. To the static pressure the profile obtained is similar to the three turbulence models. At first time it is constant in the curvature, develops a higher value on the external part of the curvature and at the finish is constant, but with a lower value than the beginning. It is clear this behavior is a consequence of the curved channel.

The aim of this work was to provide the behavior of the flow that occurs in a wind tunnel located at the Fluid Mechanics Laboratory – DEM/ UFPA. Further effects, especially experimental validation are needed to improve the capacity of the models for predicting flow with complex boundary conditions.

The results in Fig. 8 shows the comparison between the numerical simulation and the experimental data.

According the contours of total pressure we observed that the behavior is very similar for the planes 0, 1, 2, 3, 4 and 5.

The experimental data were obtained trough the work realized by Ferreira and it measured at the same structure the grid which this work is based. It is important to stand out that in the wind tunnel located in DEM-UFPA there is all the planes and the numerical simulation data were obtained considering the same point of experimental data was obtained.

And the results of Fig. 9 present the contours of vorticity in 3 of 6 planes present on the numerical simulation.

These three planes are the most considerable because they are the planes in the curvature and on the exit of bend. The flows are not continuous and the motions aren't unique and it is known that the separated flows are discontinuous, but the velocities are bounded.

(a) Plane 3, on the middle of the curvature.

(b) Plane 4, on the second curvature.

(c)Plane 5, on the exit of bend.
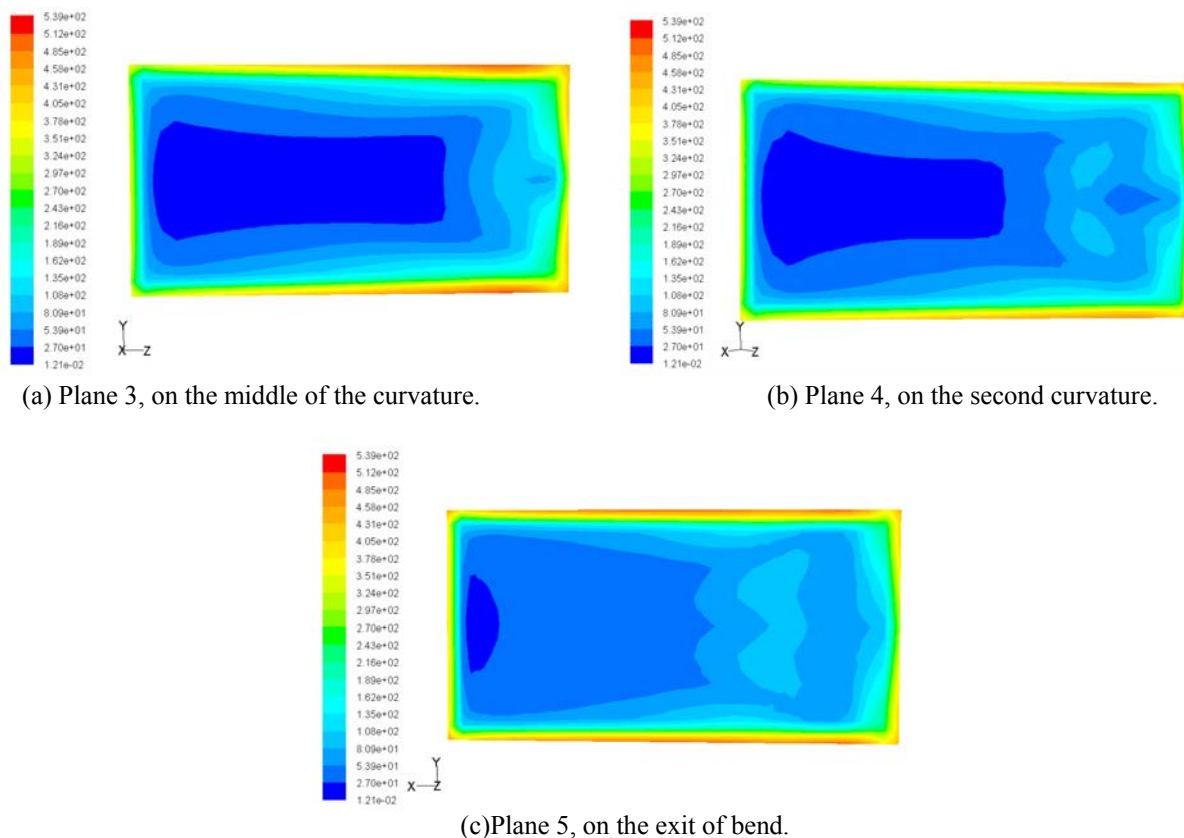
Figure 9 – The contours of vorticity magnitude predicted at the planes 3 (a), 4 (b) and 5 (c).

6. ACKNOWLEDGEMENT

7. REFERENCES

Cheng, K.C., Yuen, F.P., 1987, "Flow visualization studies on secondary flow patterns in straight tubes downstream of a 180º bend and in isothermally heated horizontal tubes", Trans. ASME, J. Heat Transfer, Vol.109, pp.49-61.
Humphrey, J. A. C., Whitelaw, J. H. and Yee, G., 1981, "Turbulent flow in a square duct with strong curvature", Journal of Fluid Mechanics, vol. 103 , pp. 443-463.
Iacovides, H., Lauber, B.E., Loizou P.A., Zhao, H.H., 1990, "Turbulent boundary-layer development around a square-sectioned U-bend: Measurements and computation." ASME, Journal of Fluids Engineering, Vol.112, pp. 409-415.
Kim W.J., Patel V.C., 1994, "Origin and decay of longitudinal vortices in developing flow in a cuved rectangular duct", Journal of Fluids Engineering, Vol.116, pp.45-52.
Shao X., Wang H., Chen Z., 2003, "Numerical modeling of turbulent flow in curved channels of compound cross section", Advances in Water Resourses, Vol.26, pp.525-539.
Schlichting, H., 1968, "Boundary-Layer Theory", McGraw-Hill, New York.
Shima N., Kawai T., Okamoto M., Tsuchikura R., 2000, "Prediction of streamline curvature effects on wall-bounded turbulent flows", International Journal of Heat and Fluid Flow, Vol.21, pp.614-619.
Silva, A.P.S., Menut P. P. P., Su J., 1998, "Turbulência", Anais da I Escola de Primavera de Transição e Turbulência.
Treaster, A.L., Yocum, A.M., 1979, "The calibration and application of five-hole probes", ISA Transactions, Vol.18, pp.23-34.
Yamamoto, K., Wu, Xiaoyun, Nozaki, K., Hayamizu, Y., 2006, "Visualization of Taylor-Dean flow in a curved duct of square cross-section", Fluid Dynamics Research, Vol.38, pp.1-18.
Winters, K.H., 1987, "A bifurcation study of laminar flow in a curved tube of rectangular cross-section", Journal Fluid Mechanics, Vol.180, pp. 343-369.

8. COPYRIGHT NOTICE